Earthq Eng & Eng Vib (2015) 14: 527-538 **DOI**: 10.1007/s11803-015-0042-1

Research on the random seismic response analysis for multi- and large-span structures to multi-support excitations

Zhao Bo[1†], Wang Yuanqing[2‡], Chen Zhihua[1‡], Shi Yongjiu[2‡], Jiang Yang[2†] and Wang Yihong[1†]

1. *School of Civil Engineering, Tianjin University, Tianjin 300072, China*
2. *Key Laboratory of Structural Engineering and Vibration of Education Ministry, Department of Civil Engineering, Tsinghua University, Beijing 100084, China*

Abstract: The pseudo excitation method (PEM) has been improved into a more practical form, on which the analytic formulae of seismic response power spectral density (PSD) of simplified large-span structural models have been derived. The analytic formulae and numerical computing results of seismic response PSD have been derived to study the mechanism of multi-support excitation effects, such as the wave-passage effect and incoherence effect, for the seismic response of multi- and large-span structures. By using a multi-span truss as an example, the influence of multi-support excitation effects on the seismic response of such structures is studied.

Keywords: random seismic response; multi-support excitations; large-span structures; wave-passage frequency; coherence function

1 Introduction

Four distinct phenomena give rise to the spatial variability of earthquake-induced ground motions (Kiureghian, 1996): (1) loss of coherency of seismic waves due to scattering in the heterogeneous medium of the ground, as well as due to the differential super positioning of waves arriving from an extended source, collectively denoted herein as the 'incoherence' effect; (2) difference in the arrival times of waves at separate stations, denoted herein as the 'wave-passage' effect; (3) gradual decay of wave amplitudes with distance due to geometric spreading and energy dissipation in the ground medium, denoted herein as the 'attenuation' effect; and (4) spatially varying local soil profiles and the manner in which they influence the amplitude and frequency content of the bedrock motion underneath each station as it propagates upward, denoted herein as the 'site-response' effect. Traditional seismic response analysis often neglects the spatial variation. In other words, the earthquake ground motions of different supports are unique. It will not produce large error when the span is small. However, for large-span building and bridge structures, the inconsistency at different supports with different excitations will lead to the structural seismic response differing from the unique excitation, so the assumption of unique input is unreasonable. The research on the earthquake response analysis of large-span structures subjected to multi-support excitations was put forward in order to study the influence of the spatial effects on these structures and ensure their safety. At present, the study of the seismic response of structures to multi-support excitations has not been fully explored. There is no perfect theoretical system and design method yet. Only the Eurocode (EN 1998-2) specifies that the spatial variation of ground motion needs to be considered in the earthquake analysis if the bridge's span exceeds a given limitation or the soil properties of a local site vary considerably. There are only a small number of tests to confirm these parameters (Yan *et al.*, 2013; Fang *et al.*, 2012) because laboratories do not yet have the capacity for such testing. As a result, the numerical computation method is the main tool used to account for this problem. The methods of analysis used for structures subjected to multi-support excitations include time-history analysis method, response spectrum method and random vibration method (Leger *et al.*, 1990; Kiureghian and Neuenhofer, 1992; Hao, 1989). More researchers prefer the random vibration method because of its statistical properties (Soyluk and Dumanoglu, 2000; Ates *et al.*, 2005; Dumanoglu and Soyluk, 2003). The Pseudo Excitation Method (Lin *et al.*, 2004; Lin and Zhang, 1992) has

Correspondence to: Chen Zhihua, School of Civil Engineering, Tianjin University, Tianjin 300072, China
Tel: +86 22 27403736; Fax: +86 22 27403736
E-mail: zhchen@tju.edu.cn
†Lecture; ‡Professor; §Assistant Professor

Supported by: National Natural Science Foundation of China under Grant No. 51038006, Specializes Research Fund for the Doctoral Program of Higher Education under Grant No. 20090002110045

Received December 15, 2013; **Accepted** July 18, 2014

sped up the promotion of the random vibration method because it solved the problem of complex theory and computation complexity of the conventional method. This study puts forward a practical solution form of the multi-support pseudo excitations method. The time item is separated, while the calculation precision is not influenced.

Many literature reviews show that the different distribution of supports results in the discrepancy of regularity of the seismic response of structures subjected to multi-support excitations. It is reasonable to study the seismic response of these structures with specific support distribution. Most of the research uses specific engineering projects to study the influence mechanism of the spatial effect, which is difficult. The single span with single mass model, as the simplified multi-support excitation model, is considered by Zhang *et al.* (2005) and Ding *et al.* (2008). The analytic formulae of the seismic response PSD considering the wave effect and incoherence effect are derived. The influence parameters of the structural response, such as wave velocity, coherence function and the span of the structure, are quantitatively analyzed. The power spectrum analytic formulae of vibration mode coordinates and internal forces for a simplified model with a single span and two mass are derived by Jiang *et al.* (2010). In addition, the excitation of different vibration modes to multi-support excitations is analyzed and the characteristics of dynamic response are studied.

In addition to structural properties, such as the span and stiffness considered in the simplified model as stated before, and that have great influence on structural response, the number of supports (or the number of spans) is also important. The more supports the structure has, the more complicated the seismic excitations become. Consequently, this study uses a simplified multi-span structure model to study the mechanism of multi-support excitation effects, including the wave-passage effect and incoherence effect, on the seismic response of multi- and large-span structures. The influence of multi-support excitation effects on the seismic response of such structures is studied by using a multi-span truss as an example.

2 Calculation method of the random seismic response to multi-support excitations

2.1 Dynamic equation of multi-support excitations

To facilitate the formula derivation later, this section first introduces the solving method of the dynamic equation of multi-support excitations (Clough and Penzien, 1993).

The general form of the dynamic equation of multi-support excitations is shown as follows:

$$\begin{pmatrix} \boldsymbol{M}_{\mathrm{ss}} & \boldsymbol{M}_{\mathrm{sb}} \\ \boldsymbol{M}_{\mathrm{bs}} & \boldsymbol{M}_{\mathrm{bb}} \end{pmatrix}\begin{pmatrix} \ddot{\boldsymbol{X}}_{\mathrm{s}} \\ \ddot{\boldsymbol{X}}_{\mathrm{b}} \end{pmatrix}+\begin{pmatrix} \boldsymbol{C}_{\mathrm{ss}} & \boldsymbol{C}_{\mathrm{sb}} \\ \boldsymbol{C}_{\mathrm{bs}} & \boldsymbol{C}_{\mathrm{bb}} \end{pmatrix}\begin{pmatrix} \dot{\boldsymbol{X}}_{\mathrm{s}} \\ \dot{\boldsymbol{X}}_{\mathrm{b}} \end{pmatrix}+ \begin{pmatrix} \boldsymbol{K}_{\mathrm{ss}} & \boldsymbol{K}_{\mathrm{sb}} \\ \boldsymbol{K}_{\mathrm{bs}} & \boldsymbol{K}_{\mathrm{bb}} \end{pmatrix}\begin{pmatrix} \boldsymbol{X}_{\mathrm{s}} \\ \boldsymbol{X}_{\mathrm{b}} \end{pmatrix}=\begin{pmatrix} 0 \\ \boldsymbol{P}_{\mathrm{b}} \end{pmatrix} \quad (1)$$

where index s and b denote structure and foundation, respectively; $\boldsymbol{X}$ is the displacement vector; $\boldsymbol{M}$, $\boldsymbol{C}$ and $\boldsymbol{K}$ are mass, damping and stiffness matrix, respectively; and $\boldsymbol{P}_{\mathrm{b}}$ is the force of the bearing applied by the foundation. Usually the absolute displacement is distributed into pseudo-static displacement and relative dynamic displacement (with superscript s and d, respectively).

$$\begin{pmatrix} \boldsymbol{X}_{\mathrm{s}} \\ \boldsymbol{X}_{\mathrm{b}} \end{pmatrix}=\begin{pmatrix} \boldsymbol{X}_{\mathrm{s}}^{\mathrm{s}} \\ \boldsymbol{X}_{\mathrm{b}} \end{pmatrix}+\begin{pmatrix} \boldsymbol{X}_{\mathrm{s}}^{\mathrm{d}} \\ 0 \end{pmatrix} \quad (2)$$

Neglecting the items of inertial force and damping in Eq. (1) gives the following equation for the response of pseudo-static displacement by static calculation.

$$\boldsymbol{X}_{\mathrm{s}}^{\mathrm{s}}=-\boldsymbol{K}_{\mathrm{ss}}^{-1}\boldsymbol{K}_{\mathrm{sb}}\boldsymbol{X}_{\mathrm{b}}=\boldsymbol{R}\boldsymbol{X}_{\mathrm{b}},\ \boldsymbol{R}=-\boldsymbol{K}_{\mathrm{ss}}^{-1}\boldsymbol{K}_{\mathrm{sb}} \quad (3)$$

Substituting Eq. (3) into Eq. (1) and neglecting the damping of the bearing gives the dynamic equation of relative dynamic displacement response as follows:

$$\boldsymbol{M}_{\mathrm{ss}}\ddot{\boldsymbol{X}}_{\mathrm{s}}^{\mathrm{d}}+\boldsymbol{C}_{\mathrm{ss}}\dot{\boldsymbol{X}}_{\mathrm{s}}^{\mathrm{d}}+\boldsymbol{K}_{\mathrm{ss}}\boldsymbol{X}_{\mathrm{s}}^{\mathrm{d}}=-\left(\boldsymbol{M}_{\mathrm{ss}}\boldsymbol{R}+\boldsymbol{M}_{\mathrm{sb}}\right)\ddot{\boldsymbol{X}}_{\mathrm{b}} \quad (4)$$

The pseudo-static displacement and relative dynamic displacement are obtained by Eqs. (3) and (4), and then the total displacement can be obtained by Eq. (2).

2.2 Multi-support pseudo excitation method

In the pseudo excitation method, the virtual ground acceleration and displacement excitations are first obtained according to the spatial effect of ground motion (Lin *et al.*, 2004).

$$\begin{aligned} \ddot{\tilde{\boldsymbol{U}}}_{\mathrm{b}} &= \boldsymbol{P}\exp\left(\mathrm{i}\omega t\right), \\ \tilde{\boldsymbol{U}}_{\mathrm{b}} &= -\frac{1}{\omega^2}\ddot{\tilde{\boldsymbol{U}}}_{\mathrm{b}}=-\frac{1}{\omega^2}\boldsymbol{P}\exp\left(\mathrm{i}\omega t\right) \end{aligned} \quad (5)$$

where superscript ~ representatives the virtual item, and Matrix $\boldsymbol{P}$ can be obtained by the Cholesky decomposition of seismic power spectrum matrix $\boldsymbol{S}(\mathrm{i}\omega)$ as follows:

$$\boldsymbol{S}\left(\mathrm{i}\omega\right)=\boldsymbol{P}^{*}\boldsymbol{P}^{\mathrm{T}} \quad (6)$$

Transferring the virtual ground motion into virtual acceleration and displacement of the support DOF gives:

$$\ddot{\tilde{\boldsymbol{X}}}_{\mathrm{b}} = \boldsymbol{E}\ddot{\tilde{\boldsymbol{U}}}_{\mathrm{b}} = \boldsymbol{EP}\exp(\mathrm{i}\omega t),$$
$$\tilde{\boldsymbol{X}}_{\mathrm{b}} = \boldsymbol{E}\tilde{\boldsymbol{U}}_{\mathrm{b}} = -\frac{1}{\omega^2}\boldsymbol{EP}\exp(\mathrm{i}\omega t) \tag{7}$$

$\boldsymbol{E}$ is the transformation matrix between ground motion and support DOFs which considers the type of seismic wave and the relationship between the direction of the propagation and the structure DOFs (Lin *et al.*, 2004). The formation and decomposition of multi-support ground motion power spectrum matrix is also introduced by Lin *et al.* (2004).

Substituting Eq. (7) into Eq. (3) and Eq. (4) gives:

$$\tilde{\boldsymbol{X}}_{\mathrm{s}}^{\mathrm{s}} = -\frac{1}{\omega^2}\boldsymbol{REP}\exp(\mathrm{i}\omega t) \tag{8}$$

$$\boldsymbol{M}_{\mathrm{ss}}\ddot{\tilde{\boldsymbol{X}}}_{\mathrm{s}}^{\mathrm{d}} + \boldsymbol{C}_{\mathrm{ss}}\dot{\tilde{\boldsymbol{X}}}_{\mathrm{s}}^{\mathrm{d}} + \boldsymbol{K}_{\mathrm{ss}}\tilde{\boldsymbol{X}}_{\mathrm{s}}^{\mathrm{d}} = -\left(\boldsymbol{M}_{\mathrm{ss}}\boldsymbol{R} + \boldsymbol{M}_{\mathrm{sb}}\right)\boldsymbol{EP}\exp(\mathrm{i}\omega t) \tag{9}$$

Then, substituting Eq. (8) and Eq. (9) into Eq. (2) gives the virtual displacement response as follows:

$$\tilde{\boldsymbol{X}}_{\mathrm{s}} = \tilde{\boldsymbol{X}}_{\mathrm{s}}^{\mathrm{s}} + \tilde{\boldsymbol{X}}_{\mathrm{s}}^{\mathrm{d}} \tag{10}$$

According to the principle of pseudo excitation method, the total displacement response spectrum can be written by:

$$\boldsymbol{S}_{X_{\mathrm{s}}X_{\mathrm{s}}}(\mathrm{i}\omega) = \tilde{\boldsymbol{X}}_{\mathrm{s}}^{*}\tilde{\boldsymbol{X}}_{\mathrm{s}}^{\mathrm{T}} = \left(\tilde{\boldsymbol{X}}_{\mathrm{s}}^{\mathrm{s}} + \tilde{\boldsymbol{X}}_{\mathrm{s}}^{\mathrm{d}}\right)^{*}\left(\tilde{\boldsymbol{X}}_{\mathrm{s}}^{\mathrm{s}} + \tilde{\boldsymbol{X}}_{\mathrm{s}}^{\mathrm{d}}\right)^{\mathrm{T}} \tag{11}$$

Equation (11) can be expanded as follows:

$$\begin{aligned}\boldsymbol{S}_{X_{\mathrm{s}}X_{\mathrm{s}}}(\mathrm{i}\omega) &= \left(\tilde{\boldsymbol{X}}_{\mathrm{s}}^{\mathrm{s}} + \tilde{\boldsymbol{X}}_{\mathrm{s}}^{\mathrm{d}}\right)^{*}\left(\tilde{\boldsymbol{X}}_{\mathrm{s}}^{\mathrm{s}} + \tilde{\boldsymbol{X}}_{\mathrm{s}}^{\mathrm{d}}\right)^{\mathrm{T}} \\ &= \tilde{\boldsymbol{X}}_{\mathrm{s}}^{\mathrm{s}*}\tilde{\boldsymbol{X}}_{\mathrm{s}}^{\mathrm{sT}} + \tilde{\boldsymbol{X}}_{\mathrm{s}}^{\mathrm{d}*}\tilde{\boldsymbol{X}}_{\mathrm{s}}^{\mathrm{dT}} + 2\mathrm{real}\left(\tilde{\boldsymbol{X}}_{\mathrm{s}}^{\mathrm{s}*}\tilde{\boldsymbol{X}}_{\mathrm{s}}^{\mathrm{dT}}\right) \\ &= \boldsymbol{S}_{X_{\mathrm{s}}X_{\mathrm{s}}}^{\mathrm{s}}(\mathrm{i}\omega) + \boldsymbol{S}_{X_{\mathrm{s}}X_{\mathrm{s}}}^{\mathrm{d}}(\mathrm{i}\omega) + \boldsymbol{S}_{X_{\mathrm{s}}X_{\mathrm{s}}}^{\mathrm{sd}}(\mathrm{i}\omega)\end{aligned} \tag{12}$$

where $\boldsymbol{S}_{X_{\mathrm{s}}X_{\mathrm{s}}}^{\mathrm{s}}(\mathrm{i}\omega)$, $\boldsymbol{S}_{X_{\mathrm{s}}X_{\mathrm{s}}}^{\mathrm{d}}(\mathrm{i}\omega)$ and $\boldsymbol{S}_{X_{\mathrm{s}}X_{\mathrm{s}}}^{\mathrm{sd}}(\mathrm{i}\omega)$ denote pseudo-static displacement power spectrum, the relative dynamic displacement power spectrum and the cross power spectrum of the coupled item of these two, respectively.

According to random vibration theory, structural response, such as the mean square deviation and the extreme expectation of response, can be calculated by the response power spectrum. This study adopts the extreme expectation of response (simplified as maximum value below) proposed by Davenport (1961).

2.3 Practical solution form of multi-support pseudo excitations method

In the process of theoretical derivation of the pseudo-excitation method, exp(iωt), as an artificial item, is the most important part. In Section 2.2, exp(iωt) is also a relatively independent item. It is not necessary because the time variable t does not take part in the calculation. This section will study the solving method of Eqs. (8) and (9). To simplify the solving method of the structural pseudo response and the pseudo excitation form of the bearing, the time item exp(iωt) is taken out of the solution process and a more practical solution form of the pseudo excitations method to multi-support excitation is put forward.

Equation (8) is a static calculation process, so exp(iωt) can be ignored. Then Eq. (8) can be expressed as follows:

$$\tilde{\boldsymbol{X}}_{\mathrm{s}}^{\mathrm{s}} = \underset{\sim}{\tilde{\boldsymbol{X}}}{}_{\mathrm{s}}^{\mathrm{s}}\exp(\mathrm{i}\omega t) \tag{13}$$

$$\underset{\sim}{\tilde{\boldsymbol{X}}}{}_{\mathrm{s}}^{\mathrm{s}} = -\frac{1}{\omega^2}\boldsymbol{REP} \tag{14}$$

where subscript ~ denotes the corresponding virtual item without the time item exp(iωt).

The right side of Eq. (9) is the typical harmonic excitation load. If only the steady-state response is considered, the structure response of Eq. (9) can be written as follows:

$$\tilde{\boldsymbol{X}}_{\mathrm{s}}^{\mathrm{d}} = \underset{\sim}{\tilde{\boldsymbol{X}}}{}_{\mathrm{s}}^{\mathrm{d}}\exp(\mathrm{i}\omega t) \tag{15}$$

$$\left(-\omega^2\boldsymbol{M}_{\mathrm{ss}} + \mathrm{i}\omega\boldsymbol{C}_{\mathrm{ss}} + \boldsymbol{K}_{\mathrm{ss}}\right)\underset{\sim}{\tilde{\boldsymbol{X}}}{}_{\mathrm{s}}^{\mathrm{d}} = -\left(\boldsymbol{M}_{\mathrm{ss}}\boldsymbol{R} + \boldsymbol{M}_{\mathrm{sb}}\right)\boldsymbol{EP} \tag{16}$$

Accordingly, the total response is:

$$\tilde{\boldsymbol{X}}_{\mathrm{s}} = \tilde{\boldsymbol{X}}_{\mathrm{s}}^{\mathrm{s}} + \tilde{\boldsymbol{X}}_{\mathrm{s}}^{\mathrm{d}} = \left(\underset{\sim}{\tilde{\boldsymbol{X}}}{}_{\mathrm{s}}^{\mathrm{s}} + \underset{\sim}{\tilde{\boldsymbol{X}}}{}_{\mathrm{s}}^{\mathrm{d}}\right)\exp(\mathrm{i}\omega t) = \underset{\sim}{\tilde{\boldsymbol{X}}}{}_{\mathrm{s}}\exp(\mathrm{i}\omega t) \tag{17}$$

$$\underset{\sim}{\tilde{\boldsymbol{X}}}{}_{\mathrm{s}} = \underset{\sim}{\tilde{\boldsymbol{X}}}{}_{\mathrm{s}}^{\mathrm{s}} + \underset{\sim}{\tilde{\boldsymbol{X}}}{}_{\mathrm{s}}^{\mathrm{d}} \tag{18}$$

Substituting Eq. (17) back into Eq. (11) to solve the response power spectral density gives:

$$\boldsymbol{S}_{X_{\mathrm{s}}X_{\mathrm{s}}}(\mathrm{i}\omega) = \tilde{\boldsymbol{X}}_{\mathrm{s}}^{*}\tilde{\boldsymbol{X}}_{\mathrm{s}}^{\mathrm{T}} = \underset{\sim}{\tilde{\boldsymbol{X}}}{}_{\mathrm{s}}^{*}\underset{\sim}{\tilde{\boldsymbol{X}}}{}_{\mathrm{s}}^{\mathrm{T}} \tag{19}$$

It can be seen from the above equation that $\tilde{\boldsymbol{X}}_{\mathrm{s}}$ is equivalent to $\underset{\sim}{\tilde{\boldsymbol{X}}}{}_{\mathrm{s}}$ when solving the power spectral density. Therefore, the original virtual response solving process of Eq. (8), Eq. (9) and Eq. (17) can be equivalent to the solving process of Eq. (14), Eq. (16) and Eq. (18), while the latter has nothing to do with the time item exp(iωt).

In order to correspond with the change of the solving process, the form of pseudo excitation is also transformed without the time variable.

$$\ddot{\tilde{\underset{\sim}{X}}}_{\mathrm{b}} = \boldsymbol{EP},\ \tilde{\underset{\sim}{X}}_{\mathrm{b}} = -\frac{1}{\omega^2}\boldsymbol{EP} \tag{20}$$

Thus, Eq. (14) and Eq. (16) can be expressed by transformed pseudo excitation as follows:

$$\tilde{\underset{\sim}{X}}{}_{\mathrm{s}}^{\mathrm{s}} = \boldsymbol{R}\tilde{\underset{\sim}{X}}_{\mathrm{b}} \tag{21}$$

$$\left(-\omega^2\boldsymbol{M}_{\mathrm{ss}} + \mathrm{i}\omega\boldsymbol{C}_{\mathrm{ss}} + \boldsymbol{K}_{\mathrm{ss}}\right)\tilde{\underset{\sim}{X}}{}_{\mathrm{s}}^{\mathrm{d}} = -\left(\boldsymbol{M}_{\mathrm{ss}}\boldsymbol{R} + \boldsymbol{M}_{\mathrm{sb}}\right)\ddot{\tilde{\underset{\sim}{X}}}_{\mathrm{b}} \tag{22}$$

Based on the derivation above, the practical solving process of the multi-support pseudo excitation method has been put forward as follows:

(1) Construct the pseudo excitation of the bearing without the time item according to Eq. (20)

(2) Solve Eqs. (21) and (22) to obtain the pseudo static response and relative dynamic response without the time item; then add these two to obtain the total pseudo response.

(3) Substitute the structural pseudo response without the time item into Eq. (19) to obtain the response power spectral density.

This solving process is a practical adjustment based on the theory of the multi-support pseudo excitation method. The whole process has nothing to do with time item exp(iωt), so the form is more concise and easier to program.

3 Influence mechanism of multi-support excitation effects for the seismic response of multi- and large-span structures

By using the simplified multi-span structural model as an example, the mechanism of multi-support excitation effects, including the wave-passage effect and incoherence effect, for the seismic response of multi- and large-span structures is studied.

3.1 Model and parameters

3.1.1 Structural model

A simplified n-span structural model is shown in the following figure:

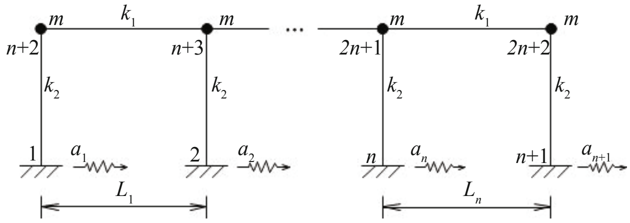

Fig. 1 Simplified structural model

The quality and stiffness of the model can refer to the gravity and natural frequency setting of the actual large-span structure: the lumped mass at the top of column m = 2.0×10^4 kg, the axial stiffness of each beam k_1 = 1000 kN/m, the lateral stiffness of each column k_2 = 400 kN/m, the structural damping ratio ζ = 0.05, the span L_i = 50 m, and $d_{ij} = \sum_{l=i}^{j-1} L_l$ denotes the spacing of bearing i and j (i, j = 1, 2, …, n+1, $i<j$).

3.1.2 Parameters of multi-support ground motion

Assume that the seismic wave propagates along the longitudinal direction and two spatial effects, the wave-passage effect and incoherence effect, are considered. Thus, two conditions are selected as follows:

Condition 1: Only wave-passage effect is considered

The incoherence effect is not considered in this condition where only the influence of the wave-passage effect is studied. The wave-passage effect is reflected by apparent wave velocity v_{app}. For convenience of analysis, the wave-passage frequency $\omega_{ij} = 2\pi v_{\mathrm{app}}/d_{ij}$ is introduced as the analysis parameter. This condition assumes the seismic ground motion of each support is completely coherent; that is, the coherence function of any two supports i and j (i, j = 1, 2, …, n+1, $i < j$) $\rho_{ij}(\omega) = 1$.

Condition 2: Both wave-passage effect and incoherence effect are considered

The influence of the incoherence effect can be further studied by comparing the calculation results between Condition 1 and Condition 2. The parameters of the wave-passage effect are the same as those of Condition 1. The incoherence effect can be reflected by the coherence function $\rho_{ij}(\omega)$. The commonly used Harichandran-Vanmarcke (simplified as H-V) coherence function model is adopted (Harichandran and Vanmarcke, 1986).

$$\begin{aligned}
&\rho_{ij}(\omega) = A\exp\left(-\frac{2d_{ij}}{\alpha\theta(\omega)}(1-A+\alpha A)\right) + \\
&(1-A)\exp\left(-\frac{2d_{ij}}{\theta(\omega)}(1-A+\alpha A)\right), \\
&\theta(\omega) = K\left[1+\left(\omega/2\pi f_0\right)^b\right]^{-1/2}; \\
&A = 0.736, \alpha = 0.147, K = 5210, \\
&f_0 = 1.09\ \text{Hz}, b = 2.78
\end{aligned} \tag{23}$$

The earthquake acceleration power spectral density function of each support is $S_a(\omega)$. This study adopts the practical power spectral model, which is synthesized by the modified response spectrum in the Chinese Code for Seismic Design of Buildings (2010). In order to ensure the rationality of the ground motion displacement characteristics, the long period segment of the response spectrum is revised (Jiang, 2010); the linear descending stage of the response spectrum is replaced by the form of T^2 with a starting period of 2 s. Assuming that there is a frequent earthquake with the fortification intensity of 7 degrees, II class site and the third design earthquake group (GB50011-2010), the synthetic ground motion acceleration power spectrum $S_a(\omega)$ and displacement power spectrum $S_u(\omega)$ are shown in Fig. 2.

3.1.3 Response of structure

This study adopts the relative displacement method, which divides the total response into a pseudo-static response and relative dynamic response to solve the dynamic equation. From the results of the analysis, it is seen that the influence mechanism of the pseudo-static response and relative dynamic response to multi-support excitations has large differences. Therefore, this research investigates the changes of the pseudo-static response, relative dynamic response and total response to study the regularity of the structural seismic response. Since the relative dynamic response to multi-support excitations has no essential differences with the dynamic response to unique excitations, the mode excitation degree can be used to reflect the relative dynamic response characteristics. The following response quantities are chosen herein to study the influence mechanism of the multi-support excitation effect.The responses of the structure include:

(1) Relative dynamic mode coordinate

The relative dynamic modal coordinate $\boldsymbol{q}_k$ directly reflects the contribution degree of the kth stage mode to relative dynamic response.

$$\boldsymbol{X}^{\mathrm{d}} = \sum_{k=1}^{N} \boldsymbol{\varphi}_k \boldsymbol{q}_k \tag{24}$$

where $\boldsymbol{X}^{\mathrm{d}}$ denotes the structural relative dynamic response, and $\boldsymbol{\varphi}_k$ denotes the kth stage mode vector.

(2) Structural internal force

The structural internal force includes the shear of column V_j and the axial force of beam F_j (i and j denote the number of columns and beams respectively, counted from left to right in Fig. 1). Each response includes the corresponding pseudo-static response, relative dynamic response and total response.

3.2 Influence of multi-support excitation effects on the structural response

3.2.1 Response power spectrum

Jiang *et al.* (2010) has studied the influence mechanism of a simplified single-span model under the multi-support excitation effect. On this basis, this section further studies the influence mechanism of a simplified two-span model to the multi-support excitation effect.

The response power spectrum of the two-span structure is derived first by the pseudo excitation method to analyze its characteristics and also calculate the maximum of response to study the change of structural seismic response under the multi-support excitations effect as the number of spans increase.

Only the pseudo-static and relativistic dynamic items are discussed herein, because the coupling term does not contribute very much to the total response. Due to space limitations, this paper only lists the typical response calculation formulae that are simple and can reflect the substantial characteristics of the structural response.

The simplified two-span structure has three modes. The natural frequency and mode are shown in Table 1. The structural parameters are as follows: $m = 2.0\times10^4$ kg, k_1=1000 kN/m, k_2=400 kN/m, $L_1 = L_2$= 50 m, ζ = 0.05.

The pseudo-static value of the beam›s axial force is equal to the corresponding value of the side-column›s shear force. Thus, only studying the pseudo-static value of the column›s axial force gives:

$$S^{\mathrm{s}}_{V_i}(\omega) = E^{\mathrm{s}}_{V_i}(\omega) k_1^2 S_u(\omega) \tag{25}$$

where $E^{\mathrm{s}}_{V_i}$ denotes the pseudo-static multi-support effect item of the ith (i = 1, 2, 3) column’s shear force.

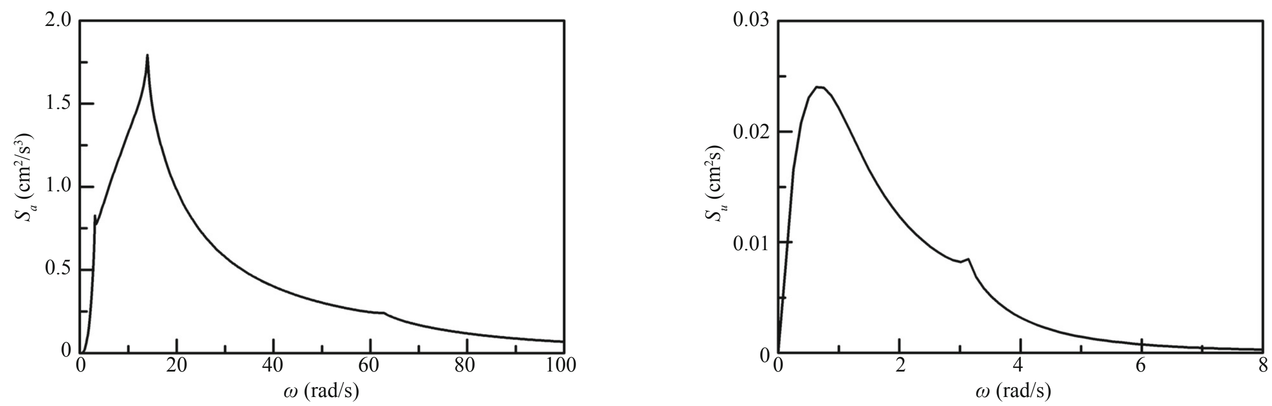

(a) Acceleration (b) Displacement

Fig. 2 Seismic power spectral density function curve

Table 1 Characteristics of simplified two-span structure

Stage	Natural frequency	Modal vector	Mode
1	$\omega_1 = \sqrt{k_2/m}$	(1, 1, 1)	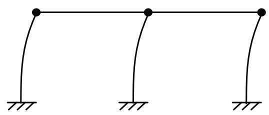
2	$\omega_2 = \sqrt{(k_1+k_2)/m}$	(1, 0, -1)	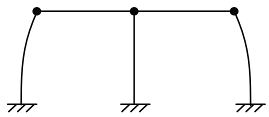
3	$\omega_3 = \sqrt{(3k_1+k_2)/m}$	(1, -2, 1)	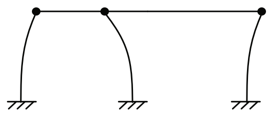

$$E^{s}_{V_1}(\omega)=\frac{2k_1^2}{(k_1+k_2)^2(3k_1+k_2)^2}\cdot \left\{(k_1+k_2)(2k_1+k_2)\left[1-\rho_{21}\cos\left(2\pi\frac{\omega}{\omega_{21}}\right)\right]+k_1(2k_1+k_2)\cdot \left[1-\rho_{31}\cos\left(2\pi\frac{\omega}{\omega_{31}}\right)\right]-k_1(k_1+k_2)\left[1-\rho_{32}\cos\left(2\pi\frac{\omega}{\omega_{32}}\right)\right]\right\} \quad (26)$$

$$E^{s}_{V_2}(\omega)=\frac{2k_1^2}{(3k_1+k_2)^2}\left\{2\left[1-\rho_{21}\cos\left(2\pi\frac{\omega}{\omega_{21}}\right)\right]-\left[1-\rho_{31}\cos\left(2\pi\frac{\omega}{\omega_{31}}\right)\right]+2\left[1-\rho_{32}\cos\left(2\pi\frac{\omega}{\omega_{32}}\right)\right]\right\} \quad (27)$$

$$E^{s}_{V_3}(\omega)=\frac{2k_1^2}{(k_1+k_2)^2(3k_1+k_2)^2}\cdot \left\{-k_1(k_1+k_2)\left[1-\rho_{21}\cos\left(2\pi\frac{\omega}{\omega_{21}}\right)\right]+k_1(2k_1+k_2)\cdot \left[1-\rho_{31}\cos\left(2\pi\frac{\omega}{\omega_{31}}\right)\right]+(k_1+k_2)(2k_1+k_2)\left[1-\rho_{32}\cos\left(2\pi\frac{\omega}{\omega_{32}}\right)\right]\right\} \quad (28)$$

The structural relative dynamic response can be reflected by vibration mode coordinates. The power spectrum of the ith (i=1, 2, 3) stage mode coordinates is:

$$S^{d}_{q_i}(\omega)=E^{d}_{q_i}(\omega)\left|H_i(\omega)\right|^2 S_a(\omega) \quad (29)$$

where $H_i(\omega)$ denotes the transfer function of the ith (i = 1, 2, 3) stage mode, and $E^{d}_{q_i}$ denotes the relative dynamic multi-support effect of the ith stage mode coordinates. Using the first stage mode as an example:

$$H_i(\omega)=\frac{1}{\omega_i^2-\omega^2+\mathrm{i}2\zeta\omega_i\omega} \quad (30)$$

$$E^{d}_{q_1}(\omega)=\frac{1}{9}\left\{3+2\rho_{21}(\omega)\cos\left(2\pi\frac{\omega}{\omega_{21}}\right)+ 2\rho_{31}(\omega)\cos\left(2\pi\frac{\omega}{\omega_{31}}\right)+2\rho_{32}(\omega)\cos\left(2\pi\frac{\omega}{\omega_{32}}\right)\right\} \quad (31)$$

$$E^{d}_{q_2}(\omega)=\frac{k_2^2}{2(k_1+k_2)^2}\left[1-\rho_{31}(\omega)\cos\left(2\pi\frac{\omega}{\omega_{31}}\right)\right] \quad (32)$$

$$E^{d}_{q_3}(\omega)=\frac{k_2^2}{18(3k_1+k_2)^2}\left\{2\left[1-2\rho_{21}(\omega)\cos\left(2\pi\frac{\omega}{\omega_{21}}\right)\right]-\left[1-\rho_{31}(\omega)\cos\left(2\pi\frac{\omega}{\omega_{31}}\right)\right]+2\left[1-\rho_{32}(\omega)\cos\left(2\pi\frac{\omega}{\omega_{32}}\right)\right]\right\} \quad (33)$$

Assigning the apparent wave velocity value v_{app}= 200 m/s, the results of the analytical expression above can be obtained as shown in Fig. 3 – Fig. 6. "wave" and "wave+incohe" in Fig. 3 and Fig. 4, respectively, denotes Condition 1 and Condition 2. Figures 5 and 6 only show the multi-support effect item of Condition 2. The influence mechanism of the multi-support effects on the structure response power spectrum can be obtained by the comprehensive analysis of each formula and each figure as follows.

(1) Any response power spectrum can be obtained by multiplying an item unrelated to the multi-support analysis and a multi-support effect item. The multi-support effect item is a trigonometric function which

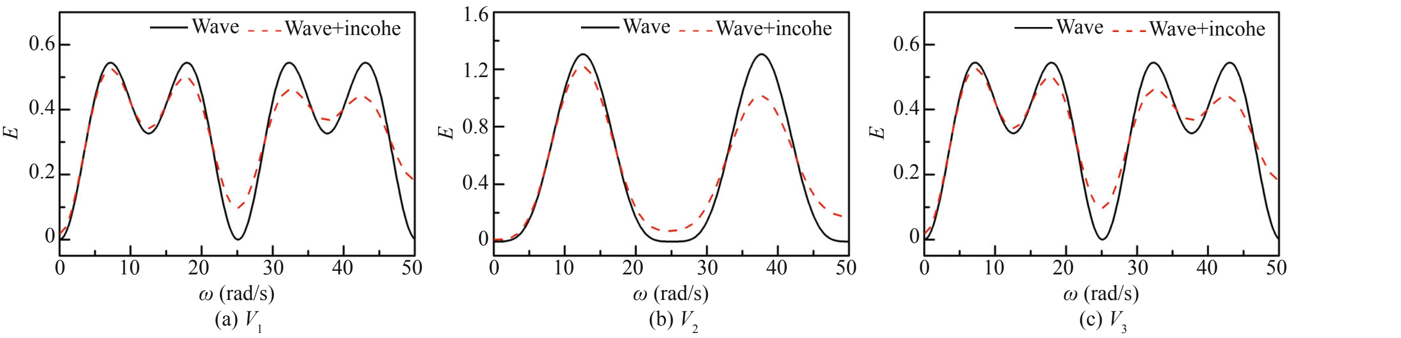

Fig. 3 Pseudo static multi-support effect items

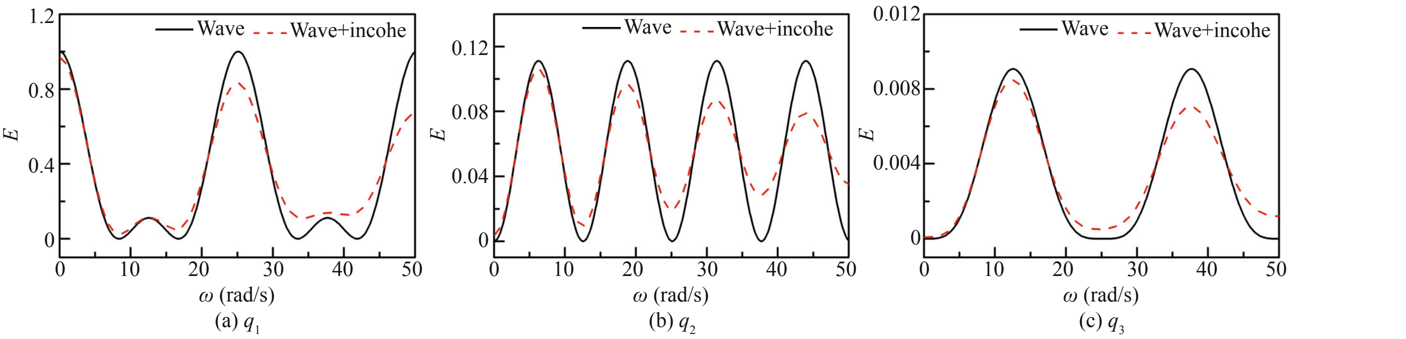

Fig. 4 Mode coordinate multi-support effect items

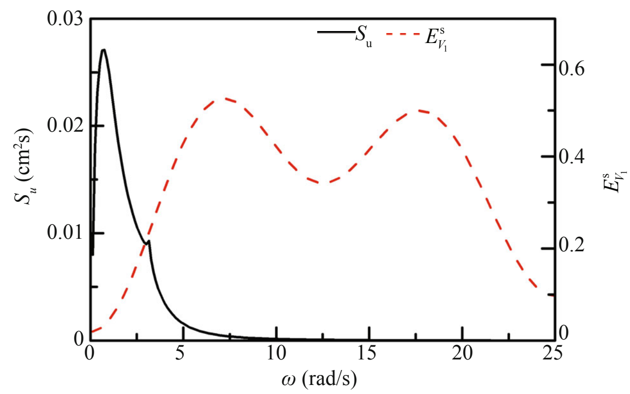

Fig. 5 Pseudo static multi-support effect item and seismic displacement power spectrum

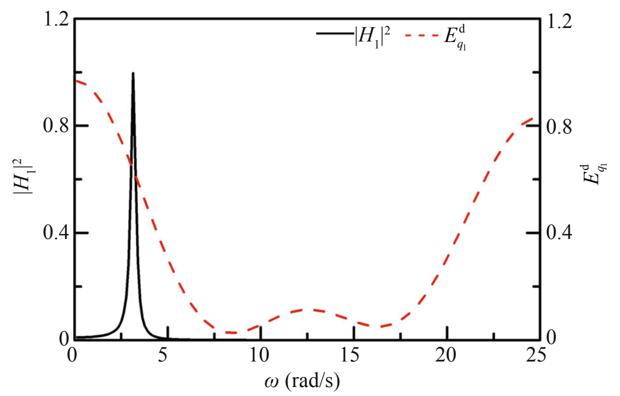

Fig. 6 Mode coordinates multi-support effect item and mode transfer function

includes wave-passage frequency ω_{ij} and incoherence function ρ_{ij}; where ω_{ij} influences the period of the function and ρ_{ij} influences the amplitude of the function.

(2) The wave-passage effect leads to the multi-support effect item as a trigonometric function distribution. All the wave-passage frequency ω_{ij} between different bearings of the multi-span structure can have an effect on the response. The multi-support effect item is superimposed by several trigonometric functions. Therefore, the period and the peak point distribution of the function become more complex, as shown in Fig. 3.

(3) The incoherence effect can decrease the amplitude of the trigonometric functions of the multi-support effect item. Due to the incoherence function, ρ_{ij} is less than 1, the amplitude of Condition 2 is less than condition 1. The greater the frequency, the higher the reduction in the amplitude.

(4) The multi-support effect item has a large distribution in the whole frequency domain, but when the other item of response analytic expression is multiplied by the distribution range of the effective value becomes small. In Fig. 5, the seismic displacement power spectrum is mainly distributed in the low frequency band, so the effective value of the pseudo static multi-support effect item is also distributed in the low frequency band. It can be seen in Fig. 6 that the mode transform function, only distributing near the natural frequency, has narrow band characteristics. Thus, when the transform function is multiplied by the multi-support effect item, only the value of the multi-support effect item near the natural frequency has a large influence on the value of the response power spectrum.

3.2.2 Extreme response

The analysis given in Section 3.2.1 shows that multi-support effects have a great influence on the relative dynamic response when the frequency variable reaches the structural natural frequency. Thus, in the analysis discussed in this section, ω_k/ω_{ij}, as independent variables, is used to consider wave velocity, where ω_k denotes the kth stage natural frequency, and ω_{ij} denotes wave-passage frequency. For the same ω_k, as ω_k/ω_{ij} becomes larger, the wave velocity will be smaller and the the wave-passage effect will be stronger. Because the influence degree of vibration mode and wave-passage frequency on different responses is diverse, the values of i, j and k should be defined in specific situation. The calculation results are shown in Fig. 7 and Fig. 8. In Fig. 8, t, d and s, respectively, denote the total response, relative dynamic response and pseudo-static response.

The figures show:

(1) In Fig. 7 and Fig. 8, the relationship between relative dynamic response and variable ω_k/ω_{ij} is shown as a trigonometric distribution. In Fig. 8, the pseudo static response monotonically increases with the variable ω_k/ω_{ij}.

(2) The wave-passage effect makes the response curves presented as trigonometric distribution. The maximum value of mode coordinates has a clear relationship with the corresponding variable ω_k/ω_{ij} as shown in Fig. 7. The distribution of peak values is obvious: when $\omega_k/\omega_{ij}=0.5m$ (m=0, 1, 2…), the corresponding mode coordinates reach the extreme. Figure 7 also shows that the wave-passage frequency ω_{21} between the adjacent bearings has the most direct influence on the 1st stage and the 3rd stage vibration mode coordinates. Meanwhile, the wave-passage frequency ω_{31} between two side bearings controls the 2nd stage vibration mode coordinate.

(3) The incoherence effect influences the amplitude of the response curve. When the variable ω_k/ω_{ij} is small, the incoherence effect is large. When the variable ω_k/ω_{ij} becomes higher, the incoherence effect becomes much smaller when compared to the wave-passage effect, and then the incoherence effect can be neglected.

(4) From the numerical values in Fig. 7, although the 2nd and 3rd stage modes are excited when considering the multi-support effect, these two mode coordinates are still much weaker than the 1st stage mode coordinate. Thus, the 1st stage mode should still be the most important influence factor on the column shear force. It also can be seen that the change law of the column relative dynamic response as shown in Fig. 8 is similar to the 1st stage relative dynamic mode coordinates in Fig. 7(a). Since the 1st stage mode cannot induce the internal forces of the beam, the change law of the beam relative dynamic response in Fig. 8 is similar to the 2nd and 3rd stage relative dynamic mode coordinates in Fig. 7.

3.3 Influence factor of the number of spans on the structural response

Assuming the number of spans is 1, 2, 3, 4, and 5, respectively, Condition 2, which considers both wave-passage effect and incoherence effect, is adopted. The internal force of Column 1, Column 2 and Beam 1 as shown in Fig. 9 – Fig. 11 are discussed in this section.

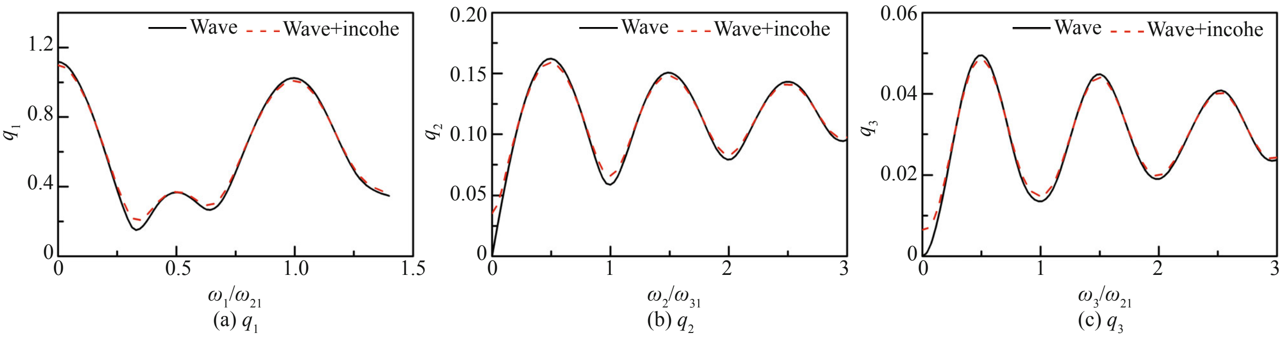

(a) q_1 (b) q_2 (c) q_3

Fig. 7 Maximum value of relative dynamic mode coordinates

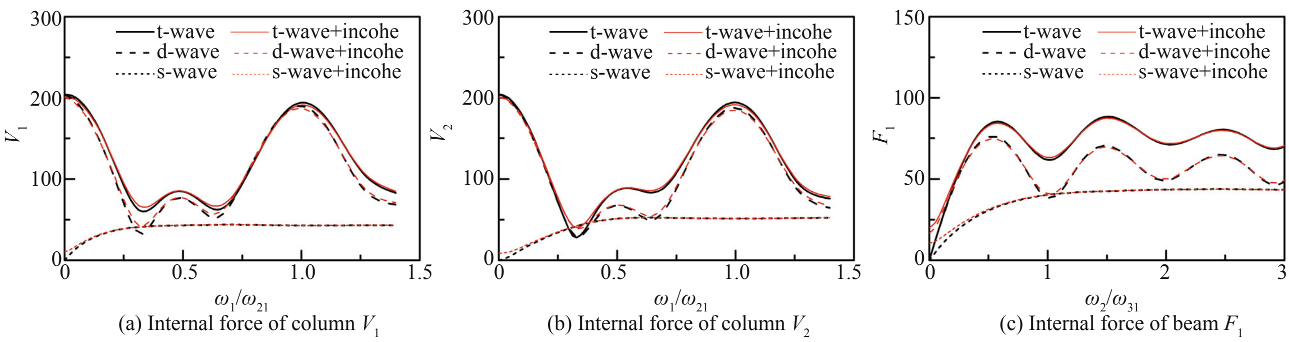

(a) Internal force of column V_1 (b) Internal force of column V_2 (c) Internal force of beam F_1

Fig. 8 Maximum value of internal force

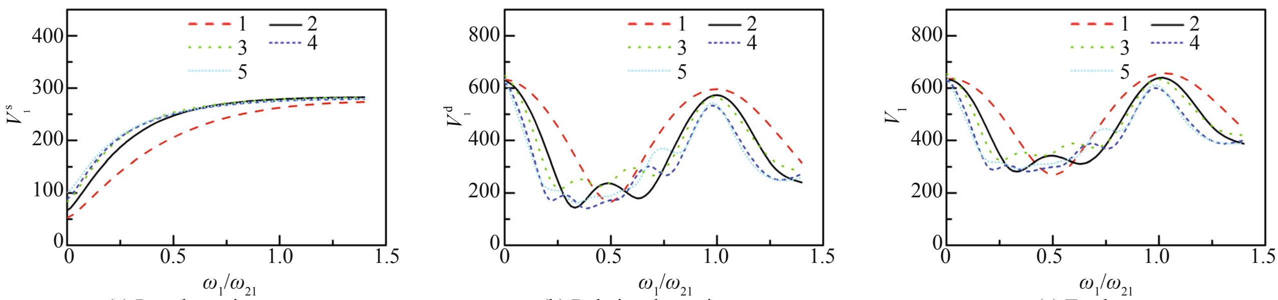

(a) Pseudo static response (b) Relative dynamic response (c) Total response

Fig. 9 Maximum value of column's Internal Force V_1

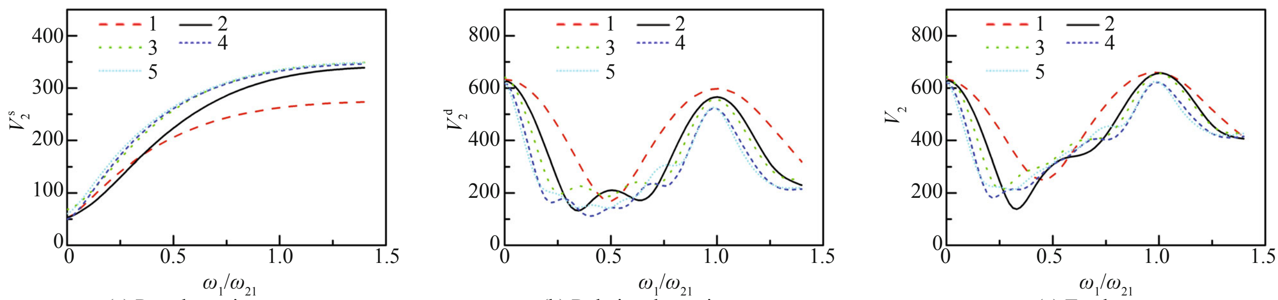

(a) Pseudo static response (b) Relative dynamic response (c) Total response

Fig. 10 Maximum value of column's Internal Force V_2

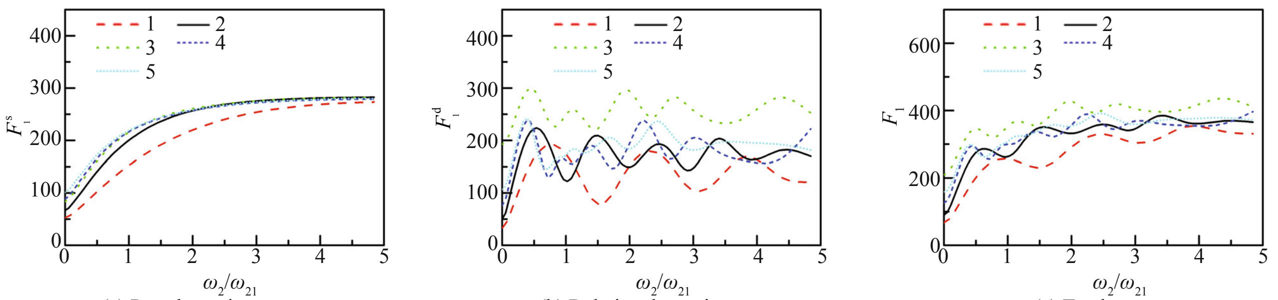

(a) Pseudo static response (b) Relative dynamic response (c) Total response

Fig. 11 Maximum value of beam's Internal Force F_1

To facilitate comparison, the abscissas of the figures are the same as those in Section 3.2.2. As the number of spans changes, the change law of structural response has obvious variations.

(1) As the number of spans is increased, the pseudo static responses of the internal force of the columns and beams also increase. When the number of span reaches 4 or 5, continued increasing number has no obvious impact on the structural pseudo static response.

(2) As the number of spans is increased, the fluctuations of the structural relative dynamic response curve become more obvious and the wave number also increases. This situation is caused by more wave-passage frequency ω_{ij} and coherence function ρ_{ij} appearing after the supports have been increased. For the structure with a different number of spans, the peak value of the internal force curves of the columns have no significant changes. However, there are differences in the peak value of the beams because the increased number of spans causes the natural frequency of the high stage vibration mode to change, which causes the corresponding variation of dynamic response.

4 Example analyses

4.1 Model and parameters

A 3-span railway station composed of a steel truss is shown in Fig. 12. The truss is supported by four rows of columns. Column 1 and Column 4 are rectangular concrete columns, and Column 2 and Column 3 are circle steel tubular columns. All the steel types adopt Q345. The seismic parameters of the site where the structure is located are listed below: 7 degree fortification intensity, II class site and the third design earthquake group (GB50011-2010). The synthetic ground motion acceleration power spectrum $S_a(\omega)$ and displacement power spectrum $S_u(\omega)$ are the same as in the previous example shown in Fig. 2.

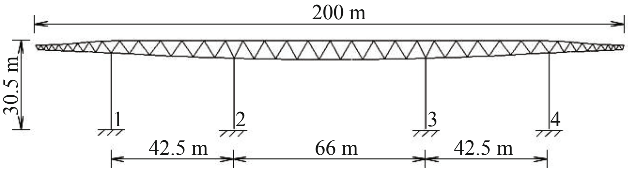

Fig. 12 Elevation of multi-span truss

Assuming that the seismic vibration direction and propagation direction are the same as the span direction, both the wave-passage effect and incoherence effect are considered. The analysis in Section 3 shows that structural responses have great fluctuation along with the variation of wave velocity, so several reasonable apparent wave velocities are adopted in the calculation. According to the fact that the equivalent shear wave velocity of this site is 300 m/s and the seismic velocity of the bedrock is over 1000 m/s, seven apparent wave velocities $v_{app} = \infty$,1600, 1000, 800, 600, 400, 300 m/s are selected. The Harichandran-Vanmarcke model (1986) as shown in Eq. (23) is used as the coherence function.

For projects in practice, the amount of the component is large and the variation of the cross sections or internal forces is great. In order to analyze the influence of the multi-support excitation effects, multi-support excitation response parameter κ is adopted:

$$\kappa = \frac{\text{multi - support excitation response}}{\text{uniform excitation response}} \tag{34}$$

4.2 Results and analysis

4.2.1 Column

The structure has bilateral symmetry, so only the shear force response of Column 1 and Column 2 with a changing wave velocity are given as shown in Fig. 13. Obviously, for the column shear force, κ is less than 1 by considering the multi-support excitation effects. Since the maximum value of the abscissa variable ω_1/ω_{41} is still less than 0.5 and the curve doesn't reach the first minimum point, the value of κ keeps reducing gradually; that is, it is safe for the column calculation without considering the multi-support excitation effect.

4.2.2 Truss member

Figure 14 shows the truss axial force distribution along the span direction. The abscissa denotes the components' center coordinates along the span direction. Obviously, multi-support excitation effects have little influence on web members but much influence on the chord members, especially when the parameter κ of the mid-span lower chord axial force has exceeded 20. For uniform excitation, the responses of these members are significantly undervalued from the study of parameter κ, and the corresponding design may be unsafe.

In order to further evaluate the structural safety with regard to multi-support excitation effects, the section stress distribution along the span direction is given in Fig. 15. The stress to uniform excitations is also showed for comparison. By comparing the curves of stress and κ value, it can be seen that the stress of the mid-span

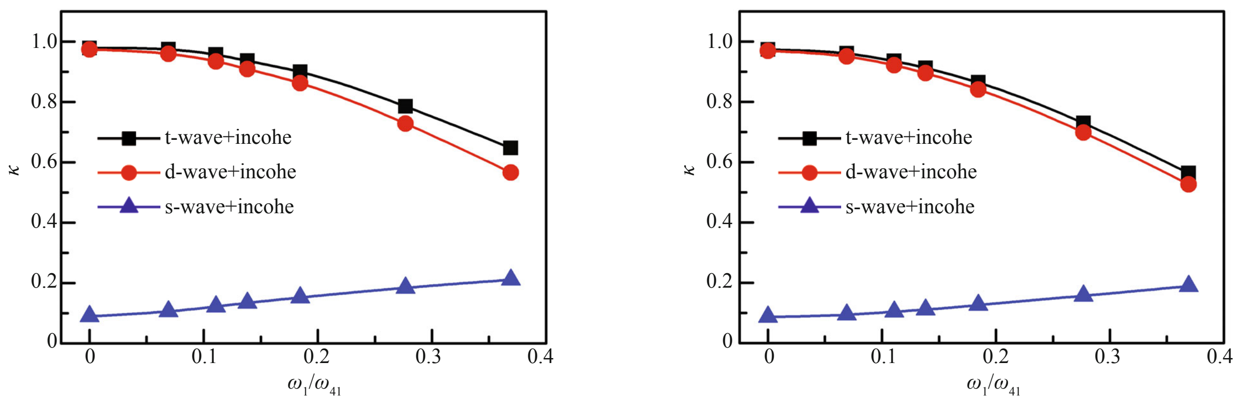

(a) Column 1 (b) Column 2

Fig. 13 Value κ of column shear force

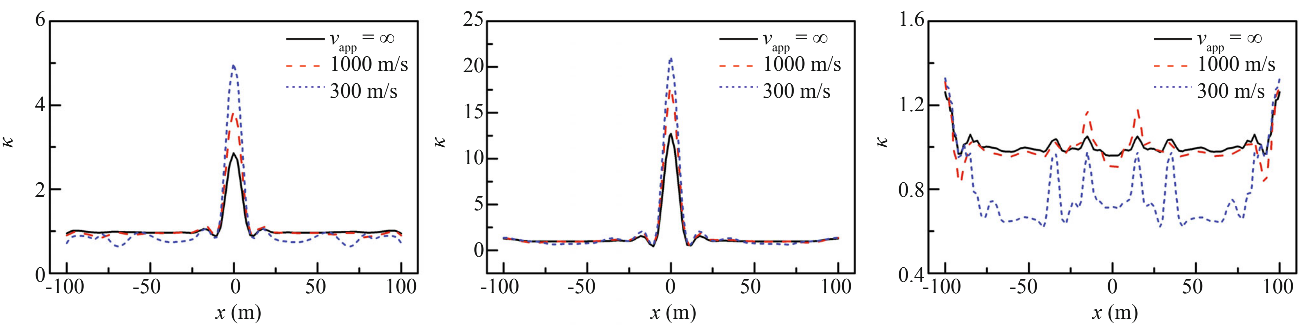

(a) Upper chord (b) Lower chord (c) Web member

Fig. 14 Value κ of truss axial force

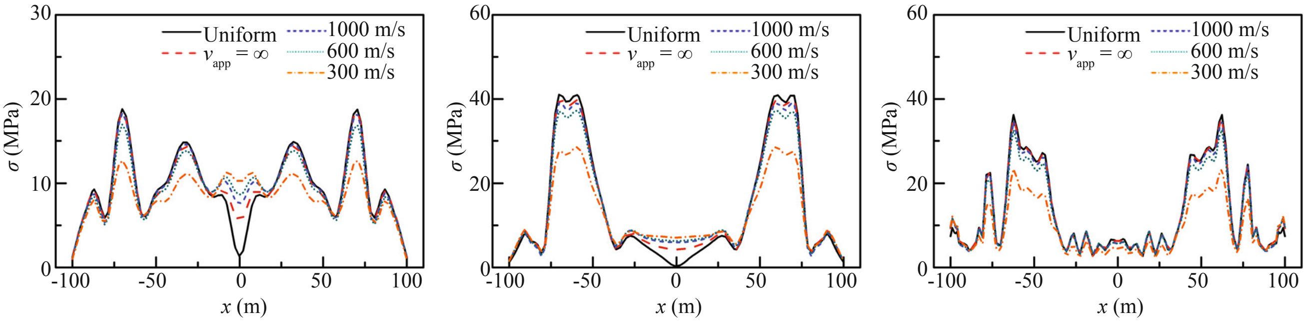

(a) Upper chord (b) Lower chord (c) Web member

Fig. 15 Truss member stress

chord caused by the earthquake is low, with a value of 10 MPa. It is much lower than the design value of material strength. The value κ of this point is large because the value of the response to uniform excitation is close to 0. The members with relatively large stress are located in the range of 50–70 m and the figure shows that the response of these members decreases after considering multi-support excitation effects with a value of κ less than 1. In conclusion, a large κ value corresponds to low stress, while a high stress corresponds to κ values of less than 1. Consequently, multi-support excitation effects have less impact on the seismic response of this kind of structure.

5 Conclusion

This study adopts several methods, such as formula derivation, numerical calculation and so on, to study the seismic response of a simplified multi-span model and multi-span truss to multi-support excitations. Both the wave-passage effect and the incoherence effect are considered. The conclusions are given as follows:

(1) The seismic response of a structure is given in the form of triangle functions by wave-passage effect and incoherence effect. The wave-passage frequency affects the function's period and the coherence function influences the amplitude attenuation.

(2) The pseudo static response increases as the number of spans is increased. When the number of spans reaches 4 or 5, a larger number of spans has little impact on the structural pseudo static response. The more spans the structure has, the more complicated the fluctuation of the relative dynamic response curve will be.

(3) If the ratio κ of the multi-support excitation response to uniform excitation response is used as the evaluation parameter, it may overestimate the influence of the multi-support excitation effects on structural safety. In order to obtain a more comprehensive evaluation, the analysis of the design parameter should be synthesized.

References

Ates S, Dumanoglu AA and Bayraktar A (2005), "Stochastic Response of Seismically Isolated Highway Bridges with Friction Pendulum Systems to Spatially Varying Earthquake Ground Motions," *Engineering Structures*, **27**(13): 1843–1858.

Clough RW and Penzien J (1993), *Dynamics of Structures*, New York: McGraw-hill College.

Davenport AG (1961), "Note on the Distribution of the Largest Value of a Random Function with Application to Gust Loading," *Proc Inst Civil Eng*, **28**: 187–196.

Ding Yang, Zhang Jiwei and Li Zhongxian (2008), "Influence of Wave Travelling Effect on Random Seismic Responses of Long-span Spatial Structures," *Journal of Earthquake Engineering and Engineering Vibration*, **4**(1): 24–31. (in Chinese)

Dumanoglu AA and Soyluk K (2003), "A Stochastic Analysis of Long Span Structures Subjected to Spatially Varying Ground Motions Including the Site-response Effect," *Engineering Structures*, **25**(10): 1301–1310.

European Committee for Standardisation (1998), *Eurocode 8: Design of Structures for Earthquake Resistance – Part 2: Bridges*, European Prestandard prEnv, Brussels.

Fang Zhenzheng, Zhang Chao, Chen Yongjian, Zheng Zequn and Xu Li (2012), "Research on the Shaking Table Test of Three Towers Cable-stayed Bridge Based on Three Shaking Table System," *China Civil Engineering Journal*, **45**: 25–29. (in Chinese)

Hao H (1989), "Effects of Spatial Variation of Ground Motions on Large Multiply-supported Structures," *Report No. UCB/EERC-89-06*, University of California at Berkeley.

Harichandran RS and Vanmarcke EH (1986), "Stochastic Variation of Earthquake Ground Motion in Space and Time," *Journal of Engineering Mechanics*, **112**(2): 154–174.

Jiang Yang (2010), "Research on the Earthquake Response Analysis and Seismic Design Methods for Large-span Building Structure," *Ph.D. Thesis*, Beijing: Tsinghua university. (in Chinese)

Jiang Yang, Shi Yongjiu and Wang Yuanqing (2010), "Analysis of Random Seismic Response of Two Supporting Plane Structures under Multi-support

Excitation," *Journal of Hunan University: Natural Sciences*, **37**(10): 13–19. (in Chinese)

Kiureghian AD (1996), "A Coherency Modal for Spatially Varying Ground Motions," *Earthquake Engineering & Structural Dynamics*, **25**(1): 99–111.

Kiureghian AD and Neuenhofer A (1992), "Response Spectrum Method for Multi-support Seismic Excitations," *Earthquake Engineering & Structural Dynamics*, **21**(8): 713–740.

Leger P, Ide IM and Paultre P (1990), "Multiple-support Seismic Analysis of Large Structures," *Computers and Structures*, **36**(6): 1153–1158.

Lin JH and Zhang WS (1992), "A Fast CQC Algorithm of PSD Matrices for Random Seismic Responses," *Computers & Structures*, **44**(3): 683–687.

Lin JH, Zhang YH, Li QS and Williams FW (2004), "Seismic Spatial Effects for Long-span Bridges, Using the Pseudo Excitation Method," *Engineering Structures*, **26**(9): 1207–1216.

National Standard of the People's Republic of China (2010), *Code for Seismic Design of Buildings* (*GB50011-2010*), Ministry of Construction of the People's Republic of China, Beijing: China. (in Chinese)

Soyluk K and Dumanoglu, AA (2000), "Comparison of Asynchronous and Stochastic Dynamic Response of a Cable-stayed Bridge," *Engineering Structures*, **22**(5): 435–445.

Yan Xiaoyu, Li Zhongxian, Han Qiang and Du Xiuli (2013), "Shaking Tables Test Study on Seismic Responses of a Long-span Rigid-framed Bridge under Multi-support Excitations," *China Civil Engineering Journal*, **46**(7): 81–89. (in Chinese)

Zhang Yahui, Li Liyuan, Chen Yan and Lin Jiahao (2005), "Wave Passage Effect on Random Seismic Response of Long-span Structures," *Journal of Dalian University of Technology*, **45**(4): 480–486. (in Chinese)